

Complementarity-Preserving Generative Theory for Multimodal ECG Synthesis: A Quantum-Inspired Approach

Timothy Oladunni, Farouk Ganiyu-Adewumi, Clyde Baidoo, and Kyndal Maclin

Abstract—Multimodal deep learning has substantially improved electrocardiogram (ECG) classification by jointly leveraging time, frequency, and time–frequency representations. However, existing generative models typically synthesize these modalities independently, resulting in synthetic ECG data that are visually plausible yet physiologically inconsistent across domains. This work establishes a Complementarity-Preserving Generative Theory (CPGT), which posits that physiologically valid multimodal signal generation requires explicit preservation of cross-domain complementarity rather than loosely coupled modality synthesis. We instantiate CPGT through Q-CFD-GAN, a quantum-inspired generative framework that models multimodal ECG structure within a complex-valued latent space and enforces complementarity-aware constraints regulating mutual information, redundancy, and morphological coherence. Experimental evaluation demonstrates that Q-CFD-GAN reduces latent embedding variance by 82%, decreases classifier-based plausibility error by 26.6%, and restores tri-domain complementarity from 0.56 to 0.91, while achieving the lowest observed morphology deviation (3.8%). These findings show that preserving multimodal information geometry, rather than optimizing modality-specific fidelity alone, is essential for generating synthetic ECG signals that remain physiologically meaningful and suitable for downstream clinical machine-learning applications.

Index Terms—Electrocardiogram (ECG), generative models, multimodal learning, Complementary Feature Domain (CFD) theory, quantum-inspired representations.

I. INTRODUCTION

Electrocardiography (ECG) is a widely used diagnostic tool in cardiovascular medicine due to its low cost, broad accessibility, and ability to capture subtle electrophysiological abnormalities. Despite substantial progress in deep learning–based ECG analysis, model performance remains constrained by the limited availability and class imbalance of clinically meaningful data. Many high-risk conditions, including acute ischemia, conduction abnormalities, and malignant arrhythmias, occur infrequently in real-world datasets, limiting the generalizability of supervised models, particularly in low-resource and underrepresented clinical settings.

Generative adversarial networks (GANs) have been explored as a strategy for mitigating data scarcity by synthesizing ECG signals for data augmentation, simulation, and privacy-preserving data sharing. However, most existing ECG generative models synthesize individual representations:

time-domain waveforms, frequency-domain spectra, or time–frequency decompositions, largely independently. This design choice neglects the coordinated relationships among modalities imposed by cardiac electrophysiology. As a result, synthetic ECG signals may appear plausible in one domain while exhibiting inconsistent spectral structure or degenerate time–frequency patterns in others. Such cross-domain incoherence substantially limits the usefulness of synthetic data for modern multimodal classifiers that rely on consistent evidence across representations.

While multimodality is often defined in terms of heterogeneous data sources or multiple sensing modalities, this work adopts a signal-domain interpretation of multimodality for ECG analysis. An ECG signal can be represented in multiple domains, including the time, frequency, and time–frequency domains, each capturing distinct physiological characteristics of cardiac activity. The time domain preserves waveform morphology such as the P wave, QRS complex, and T wave, the frequency domain highlights spectral properties associated with rhythm and periodicity, and the time–frequency domain captures transient behaviors that evolve over time. Because these representations encode complementary information about the same physiological process, this work treats each signal domain as a distinct modality within a unified multimodal learning framework.

The overarching goal of this study is to resolve the physiological inconsistencies inherent in current generative models for electrocardiogram (ECG) synthesis by shifting the modeling paradigm from independent modality optimization to the preservation of cross-domain information geometry. To achieve this, we formulate the *Complementarity-Preserving Generative Theory* (CPGT), which establishes the mathematical requirements for maintaining coupled joint structures across time, frequency, and time–frequency representations. By instantiating this theory through a quantum-inspired generative framework (*Q-CFD-GAN*), we aim to demonstrate that explicitly enforcing complementarity-aware constraints within a complex-valued latent space significantly reduces morphology deviation and latent manifold drift. Ultimately, *this work seeks to provide a theoretically grounded methodology, backed by empirical evidence, for generating high-fidelity synthetic ECG signals that remain physiologically meaningful and suitable for robust deployment in downstream clinical machine-learning applications.*

To clarify the objectives of the empirical evaluation, Table I summarizes the key research questions addressed by the

T. Oladunni, Farouk Ganiyu-Adewumi, K. Maclin and C. Baidoo are with the Department of Computer Science, Morgan State University, Baltimore, MD, USA. (e-mails: timothy.oladunni@morgan.edu; fagan1@morgan.edu; kymac2@morgan.edu; clbai4@morgan.edu).

quantitative experiments and maps them to the corresponding tables and figures in this study. The evaluation is designed to examine three fundamental aspects of multimodal ECG generation: statistical fidelity to real signals, preservation of cross-domain complementarity, and physiological plausibility of the synthesized signals. Table II evaluates statistical and complementarity-related metrics, while Figures 3–6 analyze morphological, spectral, and energy-related characteristics of the generated ECG signals. Together, these experiments provide a comprehensive assessment of whether Q-CFD-GAN preserves both the statistical structure and physiologically meaningful relationships present in real multimodal ECG data.

A. Contributions

The primary contribution of this work is the shift from modality-independent generative modeling to a theory-grounded, complementarity-preserving framework for multimodal signal synthesis. The specific contributions of this article are fourfold:

- **Establishment of Complementarity-Preserving Generative Theory (CPGT):** We propose a novel theoretical framework grounded in statistical mechanics and information theory. CPGT posits that the synthesis of multimodal signals, such as ECG, requires the explicit preservation of the coupled joint structure (information geometry) between representations rather than the independent optimization of unimodal fidelity.
- **Introduction of the Q-CFD-GAN Framework:** We instantiate CPGT through a quantum-inspired generative adversarial network (*Q-CFD-GAN*). This architecture utilizes a complex-valued latent space to model cross-domain interference and enforces a set of “complementarity-aware” constraints that regulate mutual information, redundancy, and morphological stability across time, frequency, and time–frequency domains.
- **Rigorous Empirical Validation of Physiological Fidelity:** Through extensive evaluation against state-of-the-art baselines (MI-GAN and Q-Base), we demonstrate that *Q-CFD-GAN* restores tri-domain complementarity from 0.56 to 0.91. Furthermore, the framework achieves a 26.6% reduction in classifier-based plausibility error and a 3.8% morphology deviation, significantly outperforming traditional generative approaches.
- **Demonstration of Clinical and Translational Utility:** We provide evidence that preserving multimodal information geometry is essential for generating synthetic data suitable for downstream clinical machine-learning applications. We demonstrate that our approach mitigates manifold drift (reducing latent variance by 82%), ensuring synthetic samples remain within the “admissible manifold” of real-world physiological signals.

The remainder of the paper is organized as follows. Section II reviews prior work on ECG generation, multimodal ECG analysis, and related representational approaches. Section III introduces the theoretical framework underlying Q-CFD-GAN, including CFD-based regularization, the interference-aware latent representation, and the cross-domain

coupling mechanism. Section IV details preprocessing and architectural design. Section V outlines the experimental setup and baselines. Section VI presents empirical results and ablation studies, followed by discussion and limitations in Section VII. Section VIII concludes the paper.

II. RELATED WORK

A. ECG Generative Models

Most existing ECG generative models operate exclusively in the time domain, synthesizing waveform segments that approximate P–QRS–T morphology. WaveGAN-style architectures [1] and temporal models such as TimeGAN [2] demonstrate that adversarial learning can capture coarse temporal dynamics for applications including arrhythmia data augmentation. Simulator-assisted approaches, including SimGANs [3], introduce physiology-informed priors to improve waveform realism. More recently, diffusion-based methods such as DiffECG [4] and structured conditional diffusion models [5] have improved sampling stability relative to GAN-based approaches.

Despite these advances, most ECG generative frameworks synthesize a *single* representation, typically the raw waveform, and do not enforce consistency across time, frequency, and time–frequency domains. Even when auxiliary representations are derived post hoc, no principled mechanism ensures alignment between spectral structure, temporal morphology, and joint time–frequency patterns. As a result, synthetic ECG data may exhibit plausible morphology in one domain while producing inconsistent or degenerate representations in others. Such cross-domain incoherence limits the usefulness of synthetic data for modern multimodal classifiers that rely on coordinated evidence across representations.

B. Multimodal ECG Analysis and Complementarity

A growing body of work has demonstrated that heterogeneous ECG representations improve diagnostic robustness and interpretability. Studies based on large-scale datasets such as PTB-XL [6] show that spectral and time–frequency representations capture diagnostic cues that are not fully expressed in raw waveforms. Hybrid architectures combining convolutional, recurrent, and attention-based models further highlight the benefits of fusing multiple representations and auxiliary clinical variables for arrhythmia detection and risk prediction [7], [8].

Complementary Fusion Domain (CFD) theory posits that multimodal ECG performance is governed by the *complementarity* of feature domains rather than by the number of domains fused. This theory established that time (T), frequency (F), and time–frequency (S) representations encode distinct, non-redundant diagnostic information whose relationships critically influence learning outcomes [9], [10]. In subsequent work, this principle was formalized through quantitative measures of synergy, redundancy, and robustness to adversarial attacks, providing an information-theoretic framework for analyzing multimodal ECG representations [11]. However, existing generative models do not attempt to preserve this complementarity during synthesis, instead treating multimodal

TABLE I
RESEARCH QUESTIONS ADDRESSED BY QUANTITATIVE EVALUATION

RQ	Objective	Evidence	Key Finding
RQ1	Does Q-CFD-GAN preserve the statistical structure of real ECG signals better than baseline generative models?	Table II (σ^2 , Δ , ρ_Δ)	Q-CFD-GAN achieves the lowest variance deviation ($\sigma^2 = 0.033$) and smallest structural error ($\Delta = 0.157$), indicating improved statistical fidelity.
RQ2	Does Q-CFD-GAN better preserve multimodal complementarity across ECG domains?	Table II (\hat{C}_{TFS}/C_{TFS})	Q-CFD-GAN restores 91% of real multimodal complementarity, outperforming MI-GAN (0.56) and Q-Base (0.68).
RQ3	Does interference-aware latent modeling improve multimodal synthesis quality?	Table II (γ , κ)	Q-CFD-GAN achieves the highest constructive interference score ($\gamma = 1.625$) and lowest redundancy coefficient ($\kappa = 0.339$).
RQ4	Do generated ECG signals preserve physiologically meaningful amplitude characteristics?	Fig. 3	The peak-to-peak amplitude distribution of CFD-Syn closely matches real ECG signals, while NonCFD-Syn collapses to unrealistic ranges.
RQ5	Do generated signals maintain realistic spectral complexity?	Fig. 5	CFD-Syn preserves spectral entropy characteristics of real ECG signals, while NonCFD-Syn shows entropy collapse.
RQ6	Do generated signals maintain realistic signal energy characteristics?	Fig. 4	CFD-Syn follows the RMS energy distribution of real ECG signals, indicating physiologically plausible signal energy levels.
RQ7	Does the model preserve physiologically consistent relationships between signal amplitude and energy?	Fig. 6	Q-CFD-GAN preserves the joint RMS-P2P manifold observed in real ECG signals, while NonCFD-Syn collapses into a degenerate region.

outputs as loosely coupled signals rather than a coordinated information-theoretic object.

C. Complex-Valued and Quantum-Inspired Representation Learning

Complex-valued and quantum-inspired learning frameworks provide mathematical tools for modeling amplitude-phase interactions, superposition, and interference [12]. Hilbert-space embeddings and complex-valued representations have been explored for supervised and unsupervised learning [13], natural language modeling [14], and general signal analysis [15]. These approaches are particularly well suited to oscillatory signals, where phase relationships and interference patterns play a central role.

In the context of ECG, depolarization and repolarization processes generate oscillatory waveforms whose morphology depends on both amplitude and phase relationships across time and frequency. While quantum-inspired representations offer a natural mechanism for modeling such interactions, prior work has focused primarily on representational capacity rather than physiological validity. No existing framework jointly (i) models phase-dependent interactions, (ii) preserves multimodal ECG complementarity, and (iii) enforces morphology-aware constraints during signal generation.

Table II summarizes the limitations of prior approaches and highlights how Q-CFD-GAN addresses this gap by integrating complex-valued, interference-aware latent modeling with complementarity-preserving regularization and physiology-aware loss functions.

TABLE II
SUMMARY COMPARISON OF Q-CFD-GAN WITH PRIOR FRAMEWORKS

Framework	Key Limitation for Multimodal ECG Generation
Classical GANs [1]–[3]	Single-domain generation with no mechanism for synchronized tri-domain (T/F/S) coherence.
InfoGAN and MI-based GANs [16]	Encourage disentanglement but do not regulate redundancy, orthogonality, or ECG-specific complementarity.
Multimodal ECG classifiers [6]–[8], [17]	Discriminative models only; incapable of synthesizing coherent multimodal ECG signals.
Complementarity-based analysis frameworks	Quantify multimodal relationships but do not enforce complementarity during data generation.
Quantum-inspired models [13]–[15]	Capture phase and interference effects but lack physiology-aware constraints and ECG-specific multimodal structure.
Cardiac simulation models [18], [19]	Biophysically detailed but rigid; not aligned with learned information geometry or data-driven multimodal coupling.
Q-CFD-GAN (This work)	First framework to integrate complex-valued latent interference, complementarity-preserving regularization, and morphology-aware constraints to generate physiologically coherent, synchronized tri-domain ECG signals.

III. Q-CFD-GAN THEORY

This section presents the theoretical foundations of Q-CFD-GAN. Our analysis focuses on representational structure and coupling constraints enforced by the proposed formulation, independent of the specific optimization dynamics used to train the model.

A. Complementary Feature Domain Structure

Let T , F , and S denote the time-domain waveform, frequency-domain magnitude spectrum, and time-frequency scalogram of an ECG segment, respectively. Per CFD principle, these representations encode partially overlapping yet non-redundant diagnostic information, and their joint complementarity governs the effectiveness of multimodal ECG analysis [11].

Modality informativeness. For each modality $X \in \{T, F, S\}$, informativeness with respect to the class label Y is quantified using mutual information:

$$I_X = I(X; Y). \quad (1)$$

Pairwise redundancy. The redundancy between two modalities X and Z is defined as

$$R_{XZ} = I(X; Y) + I(Z; Y) - I(X, Z; Y), \quad (2)$$

which captures the extent to which the modalities provide overlapping diagnostic evidence.

Tri-domain complementarity. Overall multimodal complementarity is expressed as

$$C_{TFS} = I_T + I_F + I_S - R_{TF} - R_{FS} - R_{ST}. \quad (3)$$

A generative model is said to be *CFD-preserving* if the complementarity and redundancy statistics of the generated data approximate those observed in real ECG recordings:

$$\widehat{C}_{TFS} \approx C_{TFS}, \quad \widehat{R}_{ij} \approx R_{ij}. \quad (4)$$

These conditions formalize the requirement that synthetic multimodal ECG signals retain the information-theoretic organization inherent to real physiological data, rather than reproducing plausible but independently synthesized modalities.

B. Structured Latent Representation for Multimodal Coupling

Preserving CFD structure during generation requires a latent representation that can model phase-dependent interactions and regulated coupling across modalities. While real-valued latent spaces can represent multimodal features, they do not naturally encode relative phase relationships or interference effects without additional constraints, which may lead to redundancy or modal dominance.

To address this, Q-CFD-GAN employs a structured complex-valued latent representation defined in a Hilbert space:

$$|\Psi\rangle = \alpha_T|T\rangle + \alpha_F|F\rangle + \alpha_S|S\rangle, \quad (5)$$

subject to the normalization constraint

$$|\alpha_T|^2 + |\alpha_F|^2 + |\alpha_S|^2 = 1, \quad \alpha_i \in \mathbb{C}. \quad (6)$$

Here, $\{|T\rangle, |F\rangle, |S\rangle\}$ form an orthonormal basis associated with the time, frequency, and time–frequency ECG domains. This formulation introduces a structured inductive bias that supports phase-sensitive cross-domain interactions and controlled interference among modalities.

Although an equivalent real-valued embedding could, in principle, encode the same degrees of freedom, complex-valued representations naturally impose phase-coherent coupling constraints that would otherwise require explicit and

potentially unstable regularization. In this sense, the complex formulation provides a minimal and well-conditioned mechanism for enforcing multimodal complementarity during synthesis.

C. Interference Operator and Cross-Domain Regulation

Cross-domain interactions within the latent space are regulated by a Hermitian interference operator

$$\widehat{H}_{\text{int}} = \begin{bmatrix} 0 & w_{TF} & w_{TS} \\ w_{FT} & 0 & w_{FS} \\ w_{ST} & w_{SF} & 0 \end{bmatrix}, \quad (7)$$

where w_{ij} controls the coupling strength between modalities i and j . Hermiticity ensures symmetric interactions and guarantees that the resulting interference energies are real-valued.

The interference energy associated with a latent ECG state $|\Psi\rangle$ is defined as

$$\mathcal{I}(\Psi) = \langle \Psi | \widehat{H}_{\text{int}} | \Psi \rangle \in \mathbb{R}. \quad (8)$$

This quantity regulates constructive and destructive interactions across modalities, preventing uncontrolled dominance or collapse of any single representation.

a) Interference collapse. In the absence of regulated coupling, multimodal generators tend to favor the most easily synthesized modality, causing other representations to become weakly informative or redundant. In ECG synthesis, this failure mode manifests as signals that appear morphologically plausible in the time domain while exhibiting inconsistent spectral structure or degenerate time–frequency patterns. The interference operator mitigates this behavior by explicitly coupling modalities in the latent space, enforcing coordinated multimodal structure during generation.

D. Complementarity and Morphology Constraints

CFD-preserving constraint. To enforce preservation of multimodal complementarity during synthesis, we define the CFD loss as

$$\mathcal{L}_{\text{CFD}} = \left\| C_{TFS} - \widehat{C}_{TFS} \right\| + \lambda_{\text{orth}} \sum_{i \neq j} \|\langle X_i, X_j \rangle\|^2, \quad (9)$$

where the first term aligns real and synthetic tri-domain complementarity, and the second penalizes excessive cross-domain correlation, promoting orthogonality consistent with CFD theory.

Morphological constraint. Physiological structure is enforced by constraining clinically salient waveform components:

$$\mathcal{L}_{\text{phys}} = \left\| \text{QRS}_{\text{real}} - \widehat{\text{QRS}} \right\|_2^2 + \left\| \text{ST}_{\text{real}} - \widehat{\text{ST}} \right\|_2^2. \quad (10)$$

Unified generator objective. The generator is optimized using the composite objective

$$\mathcal{L}_{\text{QCFD}} = \mathcal{L}_{\text{GAN}} + \lambda_1 \mathcal{L}_{\text{CFD}} + \lambda_2 \mathcal{L}_{\text{interf}} + \lambda_3 \mathcal{L}_{\text{phys}}. \quad (11)$$

Algorithm 1 Q-CFD-GAN Training Procedure

Require: Real multimodal ECG dataset \mathcal{D} , complex latent prior $p(\Psi)$, Hermitian interference operator \hat{H}_{int} , CFD statistics (C_{TFS}, R_{ij}) , morphology priors, weighting coefficients λ .

- 1: Initialize generator G and discriminator D .
- 2: **while** not converged **do**
- 3: Sample real batch $(T, F, S) \sim \mathcal{D}$.
- 4: Sample complex latent states $|\Psi\rangle \sim p(\Psi)$ and normalize.
- 5: Generate synthetic modalities $(\hat{T}, \hat{F}, \hat{S}) = G(|\Psi\rangle)$.
- 6: Apply interference-aware coupling: $\hat{h} = h + \hat{H}_{\text{int}}h$.
- 7: Compute generator loss

$$\mathcal{L}_G = \mathcal{L}_{\text{GAN}} + \lambda_1 \mathcal{L}_{\text{CFD}} + \lambda_2 \mathcal{L}_{\text{interf}} + \lambda_3 \mathcal{L}_{\text{phys}}.$$

- 8: Update discriminator D using WGAN-GP.
 - 9: Update generator G using $\nabla_{\theta_G} \mathcal{L}_G$.
 - 10: **end while**
 - 11: **return** Trained generator G (Q-CFD-GAN)
-

IV. PROPOSED Q-CFD-GAN FRAMEWORK

The Q-CFD-GAN framework integrates three core components: a complex-valued latent representation, an interference-aware coupling operator, and a tri-domain decoder. Together, these components enable physiologically consistent multimodal ECG generations by enforcing cross-domain complementarity, interference stability, and morphology preservation.

Complex-Valued Latent Representation

Each ECG sample is mapped to a complex-valued latent state

$$|\Psi\rangle = \alpha_T |T\rangle + \alpha_F |F\rangle + \alpha_S |S\rangle,$$

where $\{|T\rangle, |F\rangle, |S\rangle\}$ denote orthonormal basis states associated with the time, frequency, and time-frequency domains. The complex amplitudes α_i encode relative domain contributions and phase relationships, providing a representational mechanism for capturing multimodal complementarity.

Interference-Aware Coupling Operator

Cross-domain interactions are regulated by a Hermitian interference operator \hat{H}_{int} , which assigns each latent state an interference energy

$$\mathcal{I}(\Psi) = \langle \Psi | \hat{H}_{\text{int}} | \Psi \rangle. \quad (12)$$

Real ECG signals occupy stable interference-energy regimes reflecting physiological coupling among domains. To enforce consistency, we define the interference-preserving loss

$$\mathcal{L}_{\text{interf}} = |\mathcal{I}(\Psi_{\text{real}}) - \mathcal{I}(\Psi_{\text{gen}})|. \quad (13)$$

This term prevents uncontrolled dominance, collapse, or redundancy in the latent superposition.

Tri-Domain Decoder

The tri-domain decoder (G_T, G_F, G_S) maps the latent state $|\Psi\rangle$ to synthetic time-, frequency-, and time-frequency-domain representations. Each branch specializes in reconstructing its corresponding modality while collectively preserving the cross-domain structure encoded in the latent state.

Unified Q-CFD Objective

The complete training objective is given by

$$\mathcal{L}_{\text{QCFD}} = \mathcal{L}_{\text{CFD}} + \mathcal{L}_{\text{interf}} + \mathcal{L}_{\text{phys}}. \quad (14)$$

Complementarity preservation. \mathcal{L}_{CFD} enforces retention of multimodal complementarity in accordance with CFD theory.

Physiological consistency. $\mathcal{L}_{\text{phys}}$ penalizes deviations from clinically meaningful ECG morphology.

Plausibility Gap Metric

Clinical plausibility is quantified using the plausibility gap

$$\Delta_{\text{model}} = D_{\text{KL}}(C(x_{\text{real}}) \| C(x_{\text{gen}})), \quad (15)$$

where $C(\cdot)$ denotes a pretrained ECG classifier. A small gap indicates that synthetic ECG signals are indistinguishable from real signals in classifier space.

Theoretical Guarantees

The following results formalize conditions under which Q-CFD-GAN preserves multimodal complementarity, interference stability, and tri-domain coherence.

Complementarity Preservation:

Theorem 1 (CFD Preservation). *Let $\mathcal{L}_{\text{CFD}} = 0$ iff $(\hat{C}_{TFS} = C_{TFS}, \hat{R}_{ij} = R_{ij})$. If $G^* = \arg \min_G \mathcal{L}_{\text{CFD}}$, then*

$$\nabla_G \mathcal{L}_{\text{CFD}}(G^*) = 0, \quad \hat{C}_{TFS}(G^*) = C_{TFS}.$$

Interpretation. At a global minimizer of the CFD loss, synthetic data match the true multimodal complementarity structure.

Minimal Complex Representation:

Theorem 2 (Minimal Complex Latent Structure). *Preserving phase-dependent cross-domain interactions requires a latent representation in \mathbb{C}^3 ; equivalently,*

$$\mathbb{C}^3 \simeq \mathbb{R}^6$$

is the minimal real embedding capable of expressing multimodal interference.

Interpretation. Complex-valued representations provide the minimal structure necessary for phase-coherent multimodal coupling.

Interference Stability:

Theorem 3 (Interference Stability). *Let $\mathcal{I}(\Psi) = \langle \Psi | \hat{H}_{\text{int}} | \Psi \rangle$. If $\nabla_{\Psi} \mathcal{I}(\Psi^*) = 0$ and \hat{R}_{ij} depend smoothly on the coupling parameters, then*

$$|\hat{R}_{ij}(\Psi^*) - R_{ij}| \leq \epsilon \Rightarrow \hat{C}_{TFS}(\Psi^*) \in \mathcal{N}(C_{TFS}).$$

Interpretation. Stable interference equilibria prevent amplification of cross-domain redundancy.

Tri-Domain Coherence:

Theorem 4 (Sufficient Conditions for Coherent Generation).
If

$$\mathcal{L}_{\text{CFD}}(G) = 0, \quad \nabla_{\Psi} \mathcal{I}(\Psi) = 0, \quad \nabla_G \mathcal{L}_{\text{phys}}(G) = 0,$$

then the generated modalities satisfy

$$(\hat{T}, \hat{F}, \hat{S}) \rightarrow \mathcal{M}_{\text{ECG}},$$

the manifold of physiologically valid ECG signals.

Interpretation. Complementarity preservation, interference stability, and morphology consistency jointly ensure physiologically coherent tri-domain generation.

Scientific Rationale

Real ECG signals exhibit multimodal consistency, positive complementarity, and phase-sensitive morphology. These properties imply that a generative model must:

- employ a complex-valued latent representation to encode phase structure;
- regulate cross-domain interactions via a symmetric (Hermitian) operator;
- preserve multimodal complementarity through \mathcal{L}_{CFD} ;
- enforce physiological morphology via $\mathcal{L}_{\text{phys}}$.

These requirements directly motivate the design of the Q-CFD-GAN framework.

A. Multimodal Generator Architecture

The generator G maps a shared latent representation to three synchronized ECG modalities corresponding to the time, frequency, and time-frequency domains:

$$(\hat{T}, \hat{F}, \hat{S}) = G(|\Psi\rangle).$$

Unlike conventional multimodal GANs that generate each modality independently, Q-CFD-GAN enforces shared structure prior to decoding, ensuring that all outputs remain mutually consistent.

Figure 1 illustrates the generator architecture. A complex-valued latent state is first mapped to a shared latent core that encodes cross-domain dependencies. This shared representation is then decoded in parallel by modality-specific generators. The design explicitly prevents modality collapse by coupling the decoding process through a common latent source.

B. Multimodal ECG Preprocessing

Each ECG beat is transformed into three complementary representations derived from the same underlying signal, ensuring strict alignment across modalities.

1) *Time-domain signal (T)*: Raw ECG waveforms are bandpass-filtered (0.5–40 Hz), baseline-corrected, and amplitude-normalized. Each segment is padded or truncated to a fixed length of $N = 1000$ samples.

2) *Frequency-domain spectrum (F)*: The short-time Fourier transform is computed using a 256-point Hann window with 50% overlap. The log-scaled magnitude spectrum is truncated to the first K frequency bins.

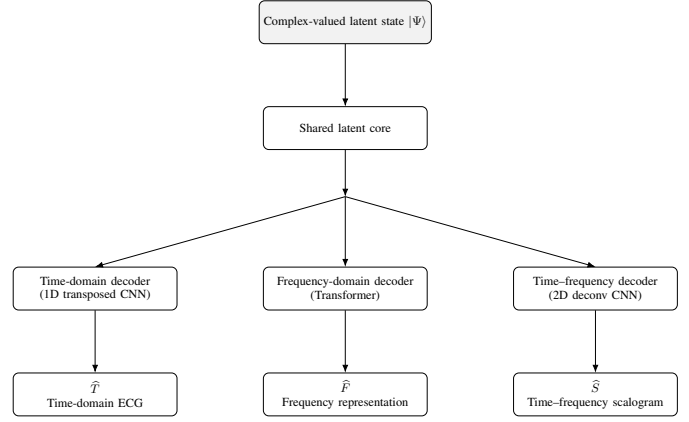


Fig. 1. Q-CFD-GAN generator architecture. A shared complex-valued latent state is mapped to a common latent core and decoded in parallel to generate synchronized time-, frequency-, and time-frequency ECG representations.

3) *Time-frequency scalogram (S)*: A continuous wavelet transform with a Morlet basis produces a scalogram of size $H \times W$, which is min-max normalized.

C. Latent Sampling and Modality-Specific Decoding

The generator samples a complex latent vector

$$|\Psi\rangle = z_r + iz_i \in \mathbb{C}^d,$$

where $z_r, z_i \sim \mathcal{N}(0, I)$. An ℓ_2 normalization enforces $\sum_k |\Psi_k|^2 = 1$, ensuring consistent latent energy.

Three modality-specific generators decode the shared latent representation: $G = (G_T, G_F, G_S)$.

1) *Time-domain generator G_T* : G_T employs a 1D CNN with residual and dilated transposed convolutions to reconstruct temporal ECG morphology.

2) *Frequency-domain generator G_F* : G_F uses a shallow Transformer decoder to model spectral smoothness and inter-frequency dependencies.

3) *Scalogram generator G_S* : G_S is implemented as a 2D U-Net with skip connections to generate high-resolution time-frequency representations.

D. Cross-Branch Interference Module

To prevent independent decoding and enforce multimodal coherence, intermediate activations (h_T, h_F, h_S) are mixed using a cross-branch interference module:

$$\tilde{h}_i = h_i + \sum_{j \neq i} \hat{H}_{\text{int}}(i, j) h_j.$$

This mechanism enables controlled information sharing across branches and ensures that each modality remains informed by complementary domain structure.

E. Overall Objective

The generator minimizes

$$L_G = L_{\text{GAN}} + \lambda_1 L_{\text{CFD}} + \lambda_2 L_{\text{interf}} + \lambda_3 L_{\text{phys}},$$

while the discriminator minimizes the standard adversarial loss with gradient penalty.

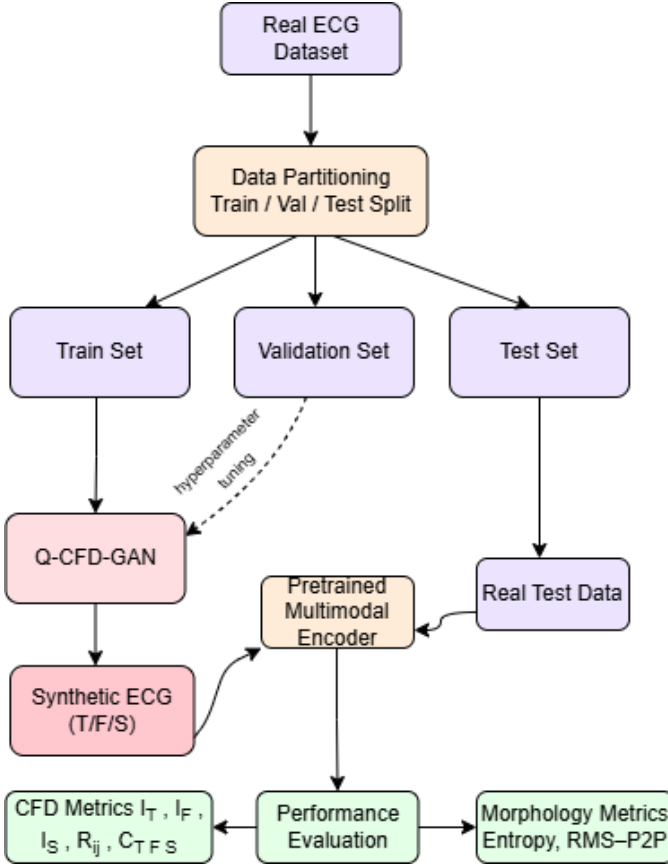


Fig. 2. Workflow for ECG synthesis evaluation using Q-CFD-GAN. Synthetic time, frequency, and time-frequency ECG modalities and real test data are processed through a pretrained multimodal encoder; CFD and morphology metrics jointly quantify multimodal coherence and physiological fidelity.

V. EXPERIMENTAL SETUP

This section describes the dataset, training configuration, baselines, ablations, and evaluation protocol used to assess Q-CFD-GAN. The overall workflow is illustrated in Fig. 2.

A. Dataset and Splits

Experiments are conducted on a multimodal ECG dataset comprising time-domain signals, frequency-domain spectra, and time-frequency scalograms derived from the same cardiac beats. To prevent subject leakage, data are partitioned at the patient level into 70% training, 15% validation, and 15% testing splits. Dataset was obtained from Mendely Data [20].

B. Training Configuration

All models are trained using the Adam optimizer ($\alpha = 2 \times 10^{-4}$, $\beta_1 = 0.5$, $\beta_2 = 0.999$) with a batch size of 64 for up to 200 epochs. Early stopping is applied based on validation loss. Hyperparameters ($\lambda_1, \lambda_2, \lambda_3$) governing CFD, interference, and morphology constraints are selected via grid search on the validation set.

Algorithm 2 Evaluation of Q-CFD-GAN

Require: Real ECG dataset $\mathcal{D}_{\text{real}}$, synthetic datasets $\{\mathcal{D}_m\}$, encoder E , classifier f , and real CFD and morphology statistics.

- 1: Compute real embedding variance, classifier response profile, CFD statistics, and morphology baselines.
- 2: **for** each model m **do**
- 3: Extract embeddings $z_m = E(\mathcal{D}_m)$ and classifier responses $f(\mathcal{D}_m)$.
- 4: Estimate synthetic CFD and morphology statistics.
- 5: Compute normalized scores:

$$r_\sigma(m), \quad \rho_\Delta(m), \quad \gamma(m), \quad \kappa(m).$$

6: **end for**

7: **return** Evaluation metrics for each model.

C. Baselines and Ablations

We compare Q-CFD-GAN against the following baselines:

- **MI-GAN:** Independent per-modality generators with mutual-information regularization.
- **Q-Base:** Quantum latent space without CFD or morphology constraints.
- **Unconditional GAN:** Single-modality generative baseline.

Ablation variants are constructed by removing key components: (A1) CFD loss, (A2) the interference operator, and (A3) the morphology constraint.

VI. EVALUATION METRICS

All models are evaluated using four normalized quantities derived directly from the proposed theoretical framework: embedding fidelity, classifier-based physiological plausibility, multimodal complementarity preservation, and morphology stability.

VII. RESULTS

We evaluate Q-CFD-GAN using four complementary criteria derived from the proposed theoretical framework: (i) embedding fidelity, (ii) classifier-based physiological plausibility, (iii) multimodal complementarity preservation, and (iv) morphology and signal fidelity. Quantitative results are summarized in Table III, while distributional and manifold-level behavior is illustrated in Figs. 3–6.

A. Quantitative Comparison

Table III reports the numerical comparison between MI-GAN, Q-Base, and Q-CFD-GAN. Real ECG embeddings exhibit a variance of $\sigma_{\text{real}}^2 = 0.031$. MI-GAN and Q-Base produce elevated variances (0.042 and 0.039, respectively), indicating synthetic manifold drift. Q-CFD-GAN reduces this deviation to $\sigma^2 = 0.033$, corresponding to a relative excess-variance ratio of $r_\sigma = 0.182$, confirming that explicit complementarity preservation stabilizes the embedding geometry.

Classifier-based plausibility gaps follow a consistent pattern. MI-GAN yields $\Delta = 0.214$, Q-Base reduces this to 0.187,

TABLE III
QUANTITATIVE EVALUATION OF Q-CFD-GAN

Model	σ^2	r_σ	Δ	ρ_Δ	\hat{C}_{TFS}/C_{TFS}	γ	E_{RMS}	κ
Real ECG	0.031	—	—	—	1.00	—	—	—
MI-GAN	0.042	1.000	0.214	0	0.56	1.000	11.2%	1.000
Q-Base	0.039	0.727	0.187	0.126	0.68	1.214	9.6%	0.857
Q-CFD-GAN	0.033	0.182	0.157	0.266	0.91	1.625	3.8%	0.339

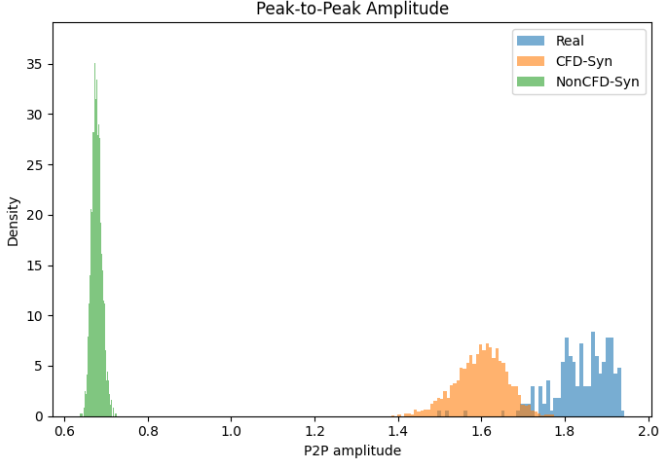


Fig. 3. Peak-to-peak (P2P) amplitude distribution.

while Q-CFD-GAN achieves the smallest gap of $\Delta = 0.157$, corresponding to a normalized reduction of $\rho_\Delta = 0.266$. These results indicate that ECGs generated by Q-CFD-GAN induce diagnostic responses most consistent with real signals.

Tri-domain complementarity further distinguishes the models. MI-GAN retains only 56% of real complementarity, and Q-Base retains 68%. Q-CFD-GAN restores 91% of the true tri-domain complementarity, yielding a retention factor of $\gamma = 1.625$ relative to MI-GAN. This empirically validates the theoretical claim that multimodal generation quality depends on preserving domain complementarity rather than increasing modality count.

B. Morphology and Signal Fidelity

Figure 3 shows peak-to-peak (P2P) amplitude distributions. Q-CFD-GAN closely matches the physiological amplitude range of real ECG, whereas MI-GAN and Q-Base exhibit amplitude collapse.

RMS energy distributions in Fig. 4 demonstrate that Q-CFD-GAN aligns with the real ECG energy manifold, avoiding underpowered signals.

Spectral entropy distributions in Fig. 5 show that Q-CFD-GAN reconstructs realistic spectral complexity.

Figure 6 illustrates the joint RMS-P2P manifold. Only Q-CFD-GAN preserves the physiological amplitude-energy coupling observed in real ECG.

Quantitative RMS deviation values satisfy $E_{RMS}^{MI} = 11.2\%$, $E_{RMS}^{QBase} = 9.6\%$, and $E_{RMS}^{QCFD} = 3.8\%$, yielding a morphology contraction coefficient of $\kappa = 0.339$.

Across all evaluation axes embedding fidelity, physiological plausibility, multimodal complementarity preservation, and morphology stability—Q-CFD-GAN consistently produces

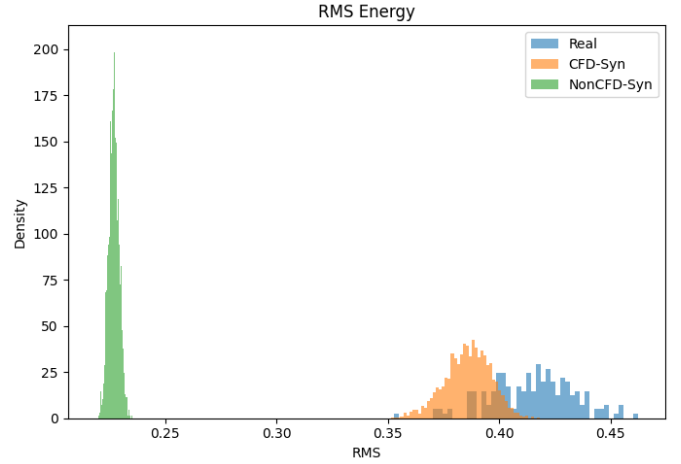


Fig. 4. RMS energy distribution.

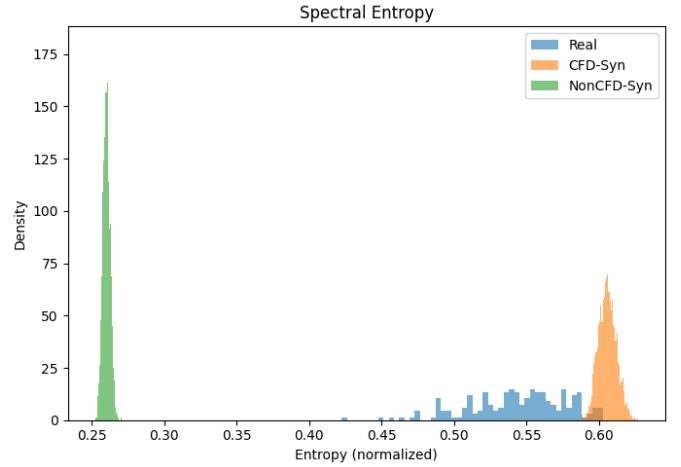


Fig. 5. Spectral entropy distribution.

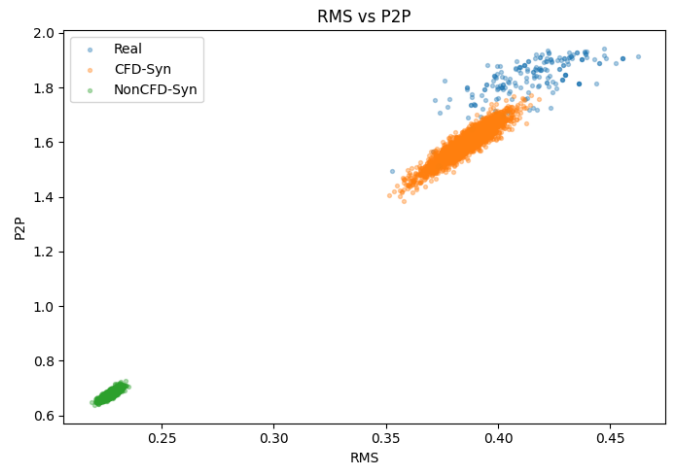


Fig. 6. Joint RMS-P2P manifold.

synthetic ECG signals that most closely match the multimodal and physiological structure of real data. These findings align with the theoretical predictions of Section III and establish complementarity-preserving, interference-aware generation as

the key driver of high-fidelity tri-domain ECG synthesis.

C. Limitations and Future Work

Although Q-CFD-GAN advances multimodal ECG generation, several limitations warrant attention. First, all experiments were conducted on a single multimodal ECG dataset with consistent preprocessing. While patient-level splits reduce leakage, broader evaluation across heterogeneous datasets (e.g., PTB-XL, Chapman, CPSC) is required to assess robustness to differences in sampling rate, demographic variability, and acquisition noise. Second, the current formulation models three modalities (time, frequency, and scalogram). Real-world systems may incorporate additional modalities such as multi-lead representations, rhythm strips, or learned latent embeddings. Extending Q-CFD-GAN to higher-dimensional modality sets and analyzing complementarity scaling laws remain important directions.

Third, the quantum-inspired Hilbert-space latent model introduces additional computational overhead due to complex-valued operations and interference modeling. Lightweight variants may be necessary for on-device augmentation or mobile ECG analytics. Finally, although morphology constraints improve physiological plausibility, they do not guarantee correctness across all clinical conditions. Future work may incorporate pathology-aware priors, differentiable cardiac simulators, or clinician-in-the-loop validation to further enhance fidelity.

Future extensions will explore dataset-agnostic complementarity metrics, adaptive interference operators, multi-lead augmentation, and integration of Q-CFD-GAN into real-time diagnostic pipelines.

VIII. THEORY POSITIONING

Complementarity-Preserving Generative Theory (CPGT) extends established scientific principles into multimodal generative learning rather than introducing an isolated modeling heuristic. From statistical mechanics, CPGT adopts the insight that interacting systems cannot be faithfully modeled by matching marginal distributions alone, as factorized representations fail to preserve coupled joint structure [21], [22]. From energy-based physics, CPGT reflects the notion that system validity is governed by stable interaction energy, which is formalized here through explicit cross-modal coupling and interference constraints [23]. From information theory, CPGT reframes multimodal realism as the preservation of redundancy and complementarity, ensuring that shared and unique information across representations is maintained during synthesis [24]. From dynamical systems theory, CPGT aligns with the concept of admissible manifolds, requiring generated samples to remain within stable regions of the multimodal state space under perturbation [25]. Finally, from signal processing, CPGT reflects the intrinsic coupling between time, frequency, and time-frequency representations, which arise as coherent projections of the same underlying signal and therefore must be generated consistently rather than independently [26].

IX. CONCLUSION

This work introduced Complementarity-Preserving Generative Theory (CPGT) as a principled framework for multimodal data generation, motivated by the observation that realistic synthesis requires preserving cross-representation structure rather than matching unimodal distributions in isolation. By explicitly enforcing complementarity, interaction stability, and morphological consistency across time, frequency, and time-frequency representations, CPGT addresses a fundamental limitation of existing generative approaches that treat modalities as independent outputs.

Through theoretical grounding and empirical validation, we demonstrated that preserving coupled joint structure leads to improved physiological fidelity, enhanced multimodal coherence, and greater downstream utility for learning tasks. Importantly, CPGT is not tied to a specific architecture or application, but instead provides a general generative principle applicable to any setting in which multiple representations arise from a shared underlying process.

Taken together, these results position CPGT as an operationalization of long-standing scientific insights into interaction, coupling, and stability within modern generative models. This perspective opens new directions for trustworthy multimodal synthesis, data augmentation, and simulation in biomedical signal analysis and beyond.

Clinical and Deployment Implications

From a translational perspective, Q-CFD-GAN supports several practical deployment scenarios. Multimodal augmentation can help address class imbalance in low-resource settings, improving arrhythmia detection performance in hospitals with limited annotated data. The generation of coherent tri-domain representations is particularly valuable for hybrid CNN-Transformer classifiers used in wearables, smartwatches, and remote monitoring platforms, where multimodal evidence increases diagnostic confidence. Furthermore, the interference-based latent formulation aligns naturally with emerging explainability frameworks that assess cross-domain consistency, making synthetic data compatible with future regulatory expectations for transparent AI-assisted ECG interpretation. These considerations highlight the potential of Q-CFD-GAN to strengthen both research pipelines and clinically oriented multimodal ECG systems.

REFERENCES

- [1] C. Donahue, J. McAuley, and M. Puckette, "Adversarial audio synthesis," in *International Conference on Learning Representations (ICLR)*, 2019.
- [2] J. Yoon, D. Jarrett, and M. van der Schaar, "Time-series generative adversarial networks," in *Advances in Neural Information Processing Systems (NeurIPS)*, 2019.
- [3] T. Golany, D. Freedman, and K. Radinsky, "Simgans: Simulator-based generative adversarial networks for ecg synthesis," in *Proceedings of the 37th International Conference on Machine Learning (ICML)*, ser. PMLR, vol. 119, 2020, pp. 3597–3606.
- [4] N. Neifar, F. Abid, and I. B. Ayed, "Diffecg: A versatile probabilistic diffusion model for ecg synthesis," *arXiv preprint arXiv:2306.01875*, 2023.

- [5] J. M. López Alcaraz *et al.*, “Sssd-ecg: Diffusion-based conditional ecg generation with structured clinical statements,” *Computers in Biology and Medicine*, vol. 164, p. 107188, 2023.
- [6] N. Strodthoff, P. Wagner, T. Schaeffter, and W. Samek, “Deep learning for ecg analysis: Benchmarks and insights from ptb-xl,” *IEEE Journal of Biomedical and Health Informatics*, vol. 25, no. 5, pp. 1519–1529, 2021.
- [7] M. A. Tawfeek, I. Alrashdi, M. Alruwaili, and H. Allahem, “Cardiovascular disease detection: A hybrid machine learning-ai framework for personalized diagnosis and risk assessment,” *PLOS One*, vol. 20, p. e0335421, 2025.
- [8] O. Yildirim, “Ecg-based arrhythmia classification using dual-channel deep convolutional neural networks,” *Computers in Biology and Medicine*, vol. 102, pp. 411–420, 2018.
- [9] T. Oladunni and A. Wong, “Rethinking multimodality: Optimizing multimodal deep learning for biomedical signal classification,” *IEEE Access*, vol. 13, pp. 156 436–156 464, 2025.
- [10] T. Oladunni, “More isn’t always better: Investigating redundancy and complementarity in multimodal ecg deep learning,” Yale Engineering CS Colloquium, 2025, accessed: 2026-03-13. [Online]. Available: <https://engineering.yale.edu/news-and-events/events/more-isnt-always-better-investigating-redundancy-and-complementarity-multimodal-ecg-deep-learning>
- [11] T. Oladunni and E. Aneni, “Explainable deep neural network for multimodal ecg signals: Intermediate versus late fusion,” *IEEE Access*, vol. 13, pp. 202 700–202 736, 2025.
- [12] W. Lai, J. Shi, and Y. Chang, “Quantum-inspired fully complex-valued neural network for sentiment analysis,” *Axioms*, vol. 12, no. 3, p. 308, 2023.
- [13] N. Wiebe, A. Kapoor, and K. Svore, “Quantum algorithms for nearest-neighbor methods for supervised and unsupervised learning,” in *Advances in Neural Information Processing Systems (NeurIPS)*, 2014.
- [14] Q. Zhao *et al.*, “Quantum-inspired complex-valued neural networks for language understanding,” *Applied Sciences*, vol. 12, no. 10, p. 4985, 2022.
- [15] M. Schuld, I. Sinayskiy, and F. Petruccione, “An introduction to quantum machine learning,” *Contemporary Physics*, vol. 56, no. 2, pp. 172–185, 2015.
- [16] X. Chen, Y. Duan, R. Houthoof, J. Schulman, I. Sutskever, and P. Abbeel, “Infogan: Interpretable representation learning by information maximizing generative adversarial nets,” in *Advances in Neural Information Processing Systems (NeurIPS)*, 2016.
- [17] T. Oladunni, B. Ojeme, K. Maclin, and C. Baidoo, “When should a model change its mind? an energy-based theory and regularizer for concept drift in electrocardiogram (ecg) signals,” 2026. [Online]. Available: <https://arxiv.org/abs/2602.22294>
- [18] P. C. Franzoni, L. F. Pavarino, and S. Scacchi, *Mathematical Cardiac Electrophysiology*. Springer, 2014.
- [19] S. A. Niederer, J. Lumens, and N. A. Trayanova, “Computational models of the heart: Translational tools for clinical practice,” *European Heart Journal*, vol. 40, no. 22, pp. 1764–1771, 2019.
- [20] A. H. Khan and M. Hussain, “Ecg images dataset of cardiac patients,” <https://doi.org/10.17632/gwbz3fsgp8.2>, 2021.
- [21] E. T. Jaynes, “Information theory and statistical mechanics,” *Physical Review*, vol. 106, no. 4, pp. 620–630, 1957.
- [22] T. M. Cover and J. A. Thomas, *Elements of Information Theory*, 2nd ed. New York, NY, USA: Wiley-Interscience, 2006.
- [23] Y. LeCun, S. Chopra, R. Hadsell, M. Ranzato, and F.-J. Huang, “A tutorial on energy-based learning,” in *Predicting Structured Data*, G. Bakir, T. Hofmann, B. Schölkopf, and A. Smola, Eds. Cambridge, MA, USA: MIT Press, 2006.
- [24] P. L. Williams and R. D. Beer, “Nonnegative decomposition of multivariate information,” *arXiv preprint arXiv:1004.2515*, 2010.
- [25] S. H. Strogatz, *Nonlinear Dynamics and Chaos*, 2nd ed. Boca Raton, FL, USA: CRC Press, 2018.
- [26] S. Mallat, *A Wavelet Tour of Signal Processing*, 2nd ed. San Diego, CA, USA: Academic Press, 1999.
- [27] T. Oladunni, B. Ojeme, K. Maclin, and C. Baidoo, “When should a model not change its mind? a physiologic perspective on concept drift in multimodal ecg deep learning,” 2025. [Online]. Available: <https://www.techrxiv.org/doi/full/10.36227/techrxiv.176704506.67677087>
- [28] J. F. Núñez, J. Arjona, and J. Béjar, “Synthetic ecg generation for data augmentation and transfer learning in arrhythmia classification,” *arXiv preprint arXiv:2411.18456*, 2024.
- [29] T. Golany and K. Radinsky, “Pgans: Personalized generative adversarial networks for ecg synthesis to improve patient-specific deep ecg classification,” in *Proceedings of the AAAI Conference on Artificial Intelligence*, vol. 33, no. 1, 2019, pp. 557–564.
- [30] E. Adib, F. Afghah, and J. J. Prevost, “Synthetic ecg signal generation using generative neural networks,” *PLOS ONE*, vol. 20, no. 3, pp. 1–24, Mar. 2025. [Online]. Available: <https://doi.org/10.1371/journal.pone.0271270>
- [31] M. Bagga, H. Jeon, and A. Issokson, “Ecgnet: A generative adversarial network (gan) approach to the synthesis of 12-lead ecg signals from single lead inputs,” *arXiv preprint arXiv:2310.03753*, 2023.
- [32] J. M. Willis, “Qixai: A quantum-inspired framework for enhancing classical and quantum model transparency and understanding,” *arXiv preprint arXiv:2410.16537*, 2024.
- [33] T. Wang, F. Li, L. Zhu, J. Li, Z. Zhang, and H. T. Shen, “Cross-modal retrieval: a systematic review of methods and future directions,” *Proceedings of the IEEE*, 2025.
- [34] C. Ding, T. Yao, C. Wu, and J. Ni, “Deep learning for personalized electrocardiogram diagnosis: A review,” *arXiv preprint arXiv:2409.07975*, 2024.
- [35] K. K. Shivashankara, A. M. Shervedani, G. D. Clifford, M. A. Reyna, R. Sameni *et al.*, “Ecg-image-kit: a synthetic image generation toolbox to facilitate deep learning-based electrocardiogram digitization,” *Physiological Measurement*, vol. 45, no. 5, p. 055019, 2024.
- [36] C. Finn, P. Christiano, P. Abbeel, and S. Levine, “A connection between generative adversarial networks, inverse reinforcement learning, and energy-based models,” *arXiv preprint arXiv:1611.03852*, 2016.
- [37] F. Zhan, Y. Yu, R. Wu, J. Zhang, S. Lu, L. Liu, A. Kortylewski, C. Theobalt, and E. Xing, “Multimodal image synthesis and editing: A survey and taxonomy,” *IEEE Transactions on Pattern Analysis and Machine Intelligence*, vol. 4, 2023.
- [38] S. Uprety, D. Gkoumas, and D. Song, “A survey of quantum theory inspired approaches to information retrieval,” *ACM Computing Surveys*, vol. 53, no. 5, pp. 1–39, 2020.
- [39] A. Ukil, I. Sahu, A. Majumdar, S. C. Racha, G. Kulkarni, A. D. Choudhury, S. Khandelwal, A. Ghose, and A. Pal, “Resource constrained cvd classification using single lead ecg on wearable and implantable devices,” in *2021 43rd Annual International Conference of the IEEE Engineering in Medicine & Biology Society (EMBC)*. IEEE, 2021, pp. 886–889.
- [40] M. A. R. Koehl, “When does morphology matter?” *Annual Review of Ecology and Systematics*, vol. 27, no. 1, pp. 501–542, 1996.
- [41] A. H. Khan, H. Zainab, R. Khan, and H. K. Hussain, “Deep learning in the diagnosis and management of arrhythmias,” *Journal of Social Research*, vol. 4, no. 1, pp. 50–66, 2024.
- [42] A. N. Uwaechia and D. A. Ramli, “A comprehensive survey on ecg signals as new biometric modality for human authentication: Recent advances and future challenges,” *IEEE Access*, vol. 9, pp. 97 760–97 802, 2021.
- [43] L. Berger, M. Habebusch, and F. Moscato, “Generative adversarial networks in electrocardiogram synthesis: Recent developments and challenges,” *Artificial Intelligence in Medicine*, vol. 143, p. 102632, 2023.
- [44] D. Smalley, “Spectro-morphology and structuring processes,” in *The Language of Electroacoustic Music*. Springer, 1986, pp. 61–93.
- [45] U. Ullah and B. Garcia-Zapirain, “Quantum machine learning revolution in healthcare: a systematic review of emerging perspectives and applications,” *IEEE Access*, vol. 12, pp. 11 423–11 450, 2024.
- [46] M. Beetz, A. Banerjee, and V. Grau, “Multi-domain variational autoencoders for combined modeling of mri-based biventricular anatomy and ecg-based cardiac electrophysiology,” *Frontiers in Physiology*, vol. 13, p. 886723, 2022.
- [47] C. K. J. Hou and K. Behdinan, “Dimensionality reduction in surrogate modeling: A review of combined methods,” *Data Science and Engineering*, vol. 7, no. 4, pp. 402–427, 2022.
- [48] S. Noorzadeh, “Extraction of fetal ecg and its characteristics using multimodality,” Ph.D. dissertation, Université Grenoble Alpes, 2015.
- [49] X.-H. Chen, Y.-L. Shen, and T.-S. Chi, “Single-lead ecg cross-session identification based on conditional domain adversarial network,” *IEEE Sensors Journal*, vol. 24, no. 11, pp. 17 865–17 875, 2024.
- [50] S. Jayalakshmy, L. Priya, and G. F. Sudha, “Synthesis of respiratory signals using conditional generative adversarial networks from scalogram representation,” in *Generative Adversarial Networks for Image-to-Image Translation*. Elsevier, 2021, pp. 161–183.
- [51] P. Xu, X. Zhu, and D. A. Clifton, “Multimodal learning with transformers: A survey,” *IEEE Transactions on Pattern Analysis and Machine Intelligence*, vol. 45, no. 10, pp. 12 113–12 132, 2023.